Chalcogenide Letters Vol. 15, No. 7, July 2018, p. 389 - 394

ON THE STRUCTURAL, OPTICAL AND MORPHOLOGICAL PROPERTIES OF $ZnSe_{1-x}O_x$ THIN FILMS GROWN BY RF-MAGNETRON SPUTTERING

S. IFTIMIE[a], F. F. BAIASU [a,b], A. RADU[a], V. A. ANTOHE[a], S. ANTOHE[a,c,*], L. ION[a]
[a]*University of Bucharest, Faculty of Physics, Bucharest, Romania*
[b]*National Institute for Laser, Plasma and Radiation Physics, Bucharest, Romania*
[c]*Academy of Romanian Scientists, Bucharest, Romania*

Thin films were grown onto optical glass substrates by magnetron sputtering in oxygen reactive atmosphere, using a zinc selenide (ZnSe) target and argon as working gas. Oxygen partial pressure was varied and the physical properties of the samples were investigated. While X-ray diffraction measurements (XRD) revealed a poor crystalline structure, scanning electron microscopy (SEM) images showed a smooth surface, free of droplets. Transmission spectra show a transmittance larger than 70% in the visible range for all fabricated $ZnSe_{1-x}O_x$ thin films, with thicknesses in the range 19 – 35 nm, as revealed by X-ray reflectometry measurements.

(Received May 18, 2018, Accepted July 17, 2018)

Keywords: Zn-Se-O compound, Magnetron sputtering

1. Introduction

Metal chalcogenide based semiconducting compounds, including among others zinc selenide (ZnSe), zinc telluride (ZnTe), cadmium sulfide (CdS) and cadmium telluride (CdTe), are suitable candidates for optoelectronic devices such as light emitting diodes (LED) and photovoltaic cells [1-5], due to their direct optical bandgap and good chemical and thermal stability. Recently, particular attention was paid to a specific class of materials, generally named zinc mono-chalcogenides, because of their abundance and low-toxicity [6,7]; e.g. ZnSe was proposed to replace CdS window layer from cadmium indium gallium selenide (CIGS) or CdTe based solar cells [8]. ZnSe is a material of interest in the field of optoelectronics because of its structural and electronic properties; in particular it has large transmittance in the infrared region of the electromagnetic spectrum. It can crystallize with cubic zinc-blende or wurtzite structure [9]. Like ZnO [10-15], ZnSe is a native n-type semiconductor and it was proved recently [16] that the ternary compound $ZnSe_{1-x}O_x$ can be obtained relatively easily. This ternary compound is interesting for optoelectronic applications, as both the bandgap width and the electric conductivity can be controlled by simply varying the oxygen fraction.

In this paper we present the results of structural, optical and morphological characterization of $ZnSe_{1-x}O_x$ thin films, prepared by rf-magnetron sputtering. While plenty of papers dedicated to ZnSe and ZnO can be found in literature, the references related to Zn-Se-O compounds are relatively scarce, irrespective of the fabrication method involved. A ZnSe target was used, the films being deposited in reactive oxygen atmosphere by varying the oxygen partial pressure.

*Corresponding author: santohe@solid.fizica.unibuc.ro

2. Experimental procedures

$ZnSe_{1-x}O_x$ thin films were fabricated by rf-magnetron sputtering onto optical glass substrates, from sintered ZnSe targets, 99.99% purity. While all the other working parameters were fixed, the oxygen (O_2) partial pressure in the deposition chamber was varied in the range $0.00 - 1.43 \times 10^{-3}$mbar. The deposition parameters used by us are summarized in Table 1. Before deposition, the glass substrates were ultrasonically cleaned in acetone and distilled water sequentially for 10 minutes. The structural, optical and morphological properties of fabricated thin layers were determined by X-ray diffraction (XRD), X-ray reflectometry (XRR), optical spectroscopy, and scanning electron microscopy (SEM), while their elemental composition was studied by energy-dispersive X-ray spectroscopy (EDX/EDS).

Table 1. Deposition parameters used for $ZnSe_{1-x}O_x$ thin films fabrication.

Sample index	Total working pressure (10^{-3} mbar)	O_2 partial working pressure (10^{-3} mbar)	Working distance (cm)	Substrate temperature (°C)	Deposition time (min)	Working power (W)
ZnSeO0	8.60	0.00	11	245	10	90
ZnSeO1	8.15	0.37	11	245	10	90
ZnSeO2	7.85	0.71	11	245	10	90
ZnSeO3	7.15	1.43	11	245	10	90

3. Results and discussions

All fabricated samples show a very poorly organized crystalline structure, as revealed by grazing incidence X-ray diffraction (GIXRD, Fig. 1). A high resolution Bruker D8 Advance diffractometer was used, with $CuK_{\alpha 1}$ radiation (λ = 1.5406 Å). The incidence angle was set to 2.5°. The broad feature at 42.5-43° is reminiscent of (220) diffraction peak of ZnSe, with a distorted lattice due to inclusion of O atoms.

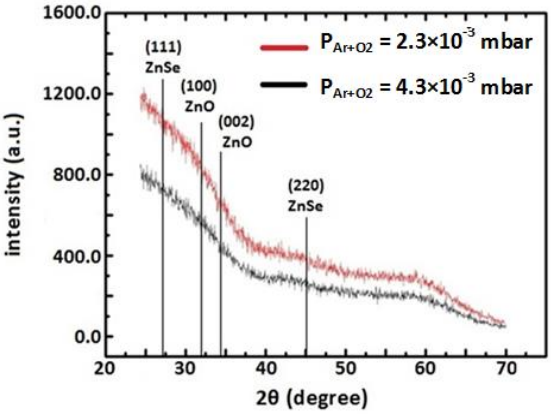

Fig. 1. GIXRD spectra recorded for two fabricated samples.

XRR was used to estimate the thickness and the roughness of the films. XRR data were fitted using the recursive Parratt-formalism [17] and the results are presented in Table 2 (see also Fig. 2). The best fit of experimental data was obtained when considering a linear variation of the density of the samples along the growth direction. In Table 2 ρ_T is the density at the surface of the film and ρ_B is the density at film/substrate interface. For comparison purposes the nominal density, ρ_N, is also indicated.

Table 2. Film parameters calculated from XRR data, using the recursive Parratt-formalism.

Sample index	O_2 partial working pressure (10^{-3} mbar)	Thickness (nm)	Roughness (nm)	ρ_T (g/cm^3)	ρ_B (g/cm^3)	ρ_N (g/cm^3)
ZnSeO0	0.00	34.6	1.70	5.23	5.32	5.26
ZnSeO1	0.37	20.8	0.65	5.09	5.21	5.26
ZnSeO2	0.71	19.2	0.49	5.11	5.31	5.26
ZnSeO3	1.43	31.6	1.37	5.11	5.31	5.26

Fig. 2 shows XRR experimental data and fitted curve for ZnSeO1 sample (the results of the fit procedure are similar for all samples).

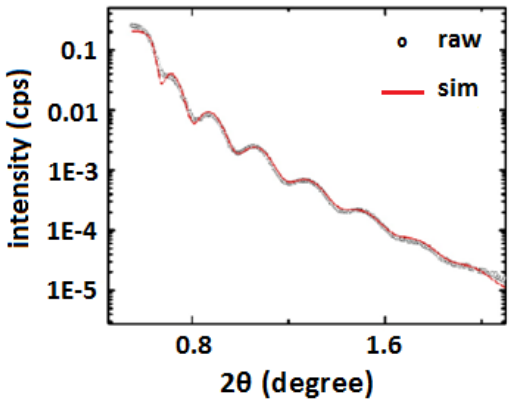

Fig. 2. Fitted XRR experimental data of fabricated ZnSeO1 sample, using t he recursive Parratt-formalism.

Except for $ZnSeO_3$, the surface roughness decreases initially with increasing O_2 partial pressure.

Optical transmission and absorption of the films were investigated using a Perkin-Elmer Lambda 35 spectrometer, in the 1100 – 200 nm spectral range, at room temperature. The optical transmission results are shown in Figure 3; except for ZnSeO0, the layers show high transmittance values in the visible range, larger than 70%. The increase of O_2 partial pressure results in the increase of transmittance in the visible range, and this behavior was noticed also in [18], being attributed to Zn-Se-O alloys produced by oxygen incorporation.

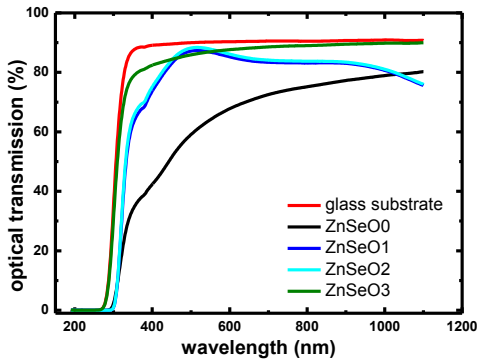

Fig. 3. Optical transmission spectra of fabricated ZnSeO0 – ZnSeO3 thin films in the wavelength ranges from 1100 to 200 nm. For comparison, the optical transmission of the substrate is presented (red curve).

The dependence of the absorption coefficient on the energy of incident photons near the fundamental threshold is shown in Fig. 4. ZnSe is a direct band gap semiconductor, and the best fit near the threshold was obtained for all the films with the well-known formula:

$$\alpha = A\frac{(\hbar\omega - E_g)^{1/2}}{\hbar\omega} \quad (1)$$

valid for direct allowed transitions. The bandgap width of the films extracted from absorption spectra using equation (1) (see Table 3) increases with the decrease of the thickness most likely due to quantum effects that became dominant.

Table 3. Calculated bandgap values of fabricated thin films.

Sample index	O_2 partial working pressure (10^{-3} mbar)	Thickness (nm)	Band gap (eV)
ZnSeO0	0.00	34.6	2.65
ZnSeO1	0.37	20.8	2.75
ZnSeO2	0.71	19.2	2.87
ZnSeO3	1.43	31.6	2.65

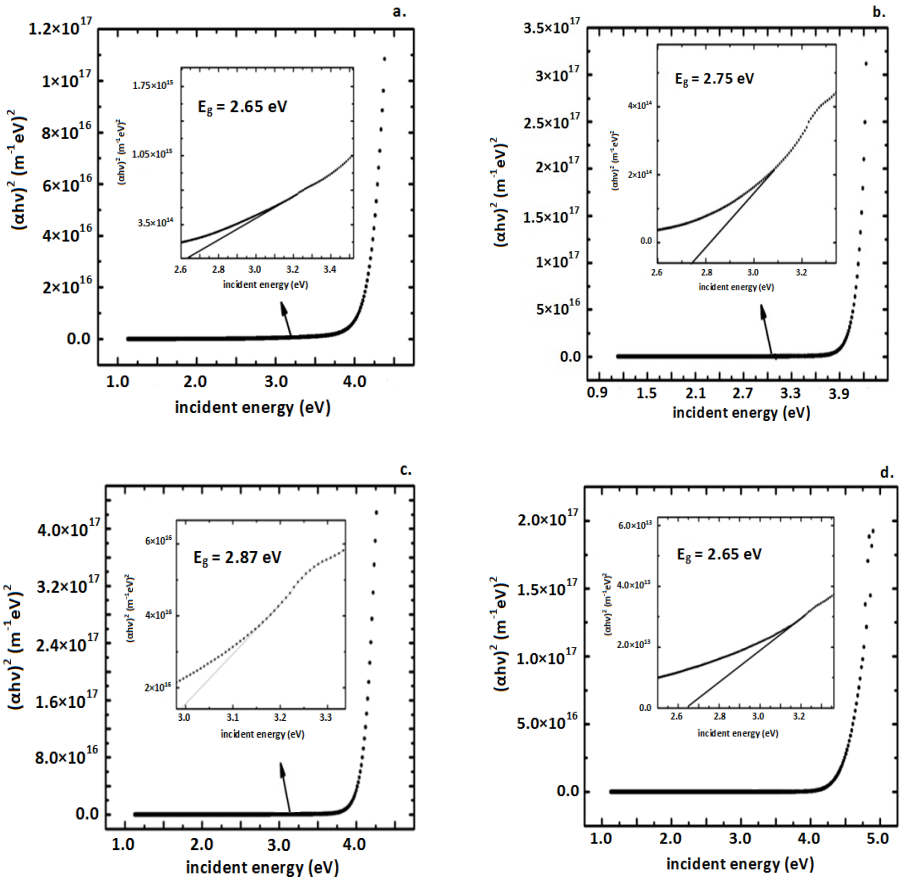

Fig. 4. Dependence of absorption coefficient on incident energy for (a) ZnSeO0, (b) ZnSeO1, (c) ZnSeO2 and (d) ZnSeO3 samples. The insets indicate the band gap values of fabricated thin layers.

The elemental composition of the samples was studied by energy-dispersive X-ray spectroscopy (EDX/EDS). Fig. 5 shows distribution maps of zinc (Zn) and selenium (Se). The decrease in Se content with increasing O_2 partial pressure may be easily observed. The morphology of the surface of the films is also changed, with increasing O_2 partial pressure. Also, no droplets were observed by SEM investigations onto the surface of prepared samples.

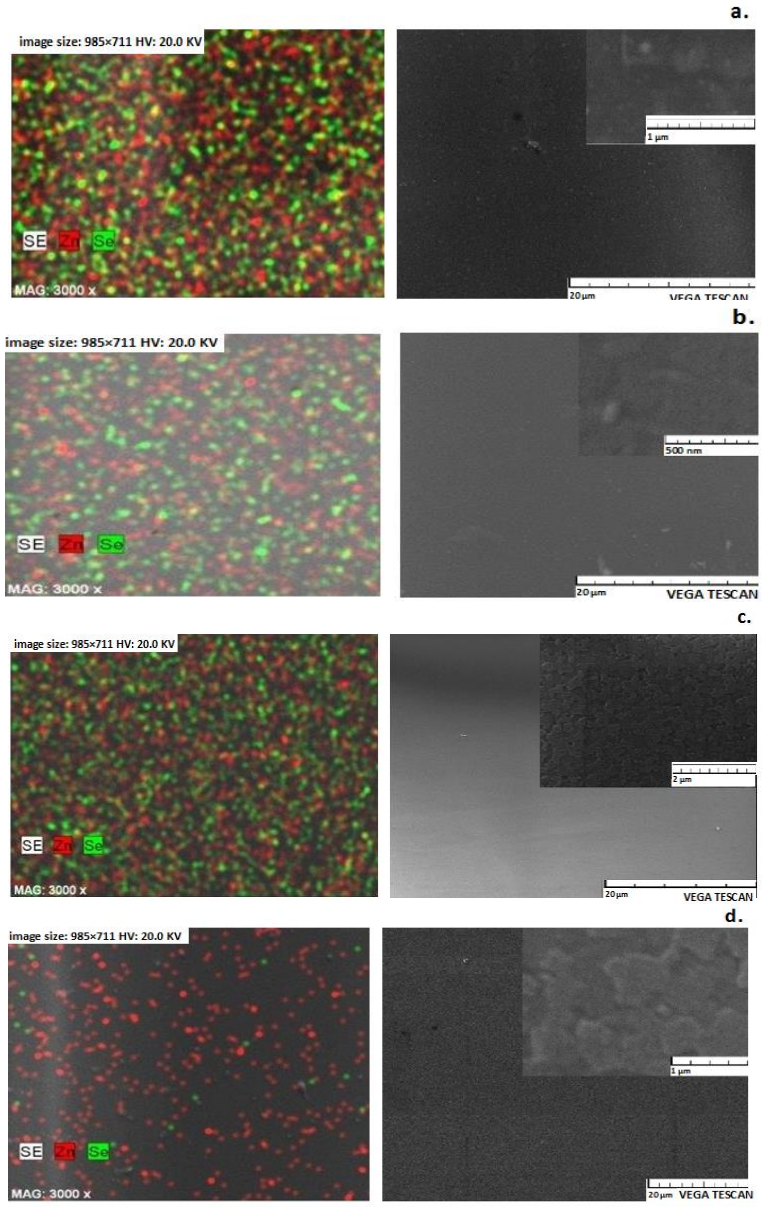

Fig. 5. The distribution maps of constitutive materials (right) and the SEM top-view images (left) of (a) ZnSeO0, (b) ZnSeO1, (c) ZnSeO2 and (d) ZnSeO3 fabricated samples.

4. Conclusions

$ZnSe_{1-x}O_x$ thin films were fabricated using a ZnSe target by reactive rf-magnetron sputtering. The control parameter was the O_2 partial pressure in the deposition chamber during growth. The crystalline structure of the films is very poor, as revealed by GIXRD investigations. SEM top-view images show a smooth surface, free of droplets.

Near threshold optical absorption spectroscopy suggests that the bandgap is direct for all the films; the bandgap width increases with the decrease of thickness, most likely due to quantum

confinement effects. With transmittance larger than 70% in the visible range, $ZnSe_{1-x}O_x$ films are suitable candidates for the fabrication of customized window layers for optoelectronic or photovoltaic applications.

Acknowledgements

This work was financially supported by FPRD project no. 18/2018 financed by UEFISCDI Romania.

References

[1] O. Toma, R. Pascu, M. Dinescu, C. Besleaga, T. L. Mitran, N. Scarisoreanu, S. Antohe, Chalcogenide Letters **8**(9), 541(2011)
[2] K. Han, S. Yoon, W. J. Chung, Interantional Journal of Applied Glass Science **6**(2), 103 (2015).
[3] S. Iftimie, C. Tazlaoanu, A. Radu, R. Constantineanu, C. Vancea, N. Korganci, L. Ion, S. Antohe, Digest Journal of Nanomaterials and Biostructures **9**(1), 213 (2014).
[4] Z. P. Weng, S. S. Ma, H. Zhu, Z. Y. Ye, T. Y. Shu, J. Zhou, X. Z. Wu, H. Z. Wu, Solar Energy Materials and Solar Cells **179**, 276 (2018).
[5] M. R. Karim, M. T. Raza, Z. A. Othman, H. A. Alturaif, N. Amin, Chalcogenide Letters **14**(10), 425 (2017).
[6] A. A. Akl. S. A. Aly, H. Howari, Chalcogenide Letters **13**(6), 247 (2016).
[7] E. Mosquera, N. Carvajal, M. Morel, C. Marin, Journal of Luminescence **192**, 814 (2017).
[8] A. Wei, X. Zhao, J. Liu, Y. Zhao, Physica B - Condensed Matter **410**, 120 (2013).
[9] A. P. Pardo Gonzalez, H. G. Castro-Lora, L. D. Lopez-Carreno, H. M. Martinez, N. J. Torres Salcedo, Journal of Physics and Chemistry of Solids **75**(6), 713 (2014).
[10] Y. Li, Y. Men, X. Kong, Z. Gao, L. Han, X. Li, Applied Surface Science **428**, 191 (2018).
[11] V. A. Antohe, L. Gence, S. K. Srivastava, L. Piraux, Nanotechnology **23**(25), 255602 (2012)
[12] I. Vaiciulis, M. Girtan, A. Stanculescu, L. Leontie, F. Habelhames, S. Antohe, Proceedings Of The Romanian Academy Series A-Mathematics Physics Technical Sciences Information Science **13**(4), 335 (2012)
[13] G. Socol, D. Craciun, N. Mihailescu, N. Stefan, C. Besleaga, L. Ion, S. Antohe, K. V. Kim, Norton, S. J. Pearton, A. C. Galca, V.Craciun, Thin Solid Films **520**(4), 1274 (2011)
[14] S. Antohe, L. Ion, V. A. Antohe, J. Optoelectron. Adv. M. **5**(4) 801 (2003)
[15] S. Antohe, L. Ion, V. A. Antohe, M. Ghenescu, J. Optoeectron. Adv. M. **9**(5), 1382 (2007)
[16] J. Sekkiou, H. Benoudnine, A. Boukortt, Y. Zidi, Optik **127**(22), 11020 (2016).
[17] D. Rafaja, H. Fuess, D. Simek, J. Kub, J. Zweck, J. Vacinova, V. Valvoda, Journal of Physics - Condensed Matter **14**(21), 5303 (2002).
[18] G. Quemard, P. Reiss, S. Carayon, J. Bleuse, Journal of Crystal Growth **275**(1-2), E2395 (2005).